

# The Development of the fragility curve for railway embankment

Divesh Ranjan Kumar <sup>a,\*</sup>, Alok Bharti <sup>a</sup>, Pijush Samui <sup>a</sup>, Sanjay Kumar <sup>a</sup> and Pradeep Kurup <sup>b</sup>

<sup>a</sup> National Institute of Technology (NIT) Patna, Bihar, India.

<sup>b</sup> Department of Civil and Environmental Engineering, University of Massachusetts Lowell, Lowell, United States.

## Article History:

Received: 22 July 2022.

Revised: 16 October 2023.

Accepted: 13 January 2024.

## ABSTRACT

For the construction of railway embankments, geotechnical engineers pay special attention to slope stability studies. The factor of safety values plays a crucial part in assessing the safe design of slopes. These values determine how close or far slopes are from failing due to natural or man-made causes. While the factor of safety is a numeric indicator of relative stability, it does not indicate the actual risk level of any structure. However, the reliability index and probability of failure quantify the risk level. The present study discusses the findings of a study to determine the factor of safety of an embankment with 12.3 m height using Geo-studio 2012 software. In this article, the fragility curve for six different types of cross-sections was also developed, i.e. the graph between the probability of failure ( $P_f$ ) and horizontal seismic coefficient ( $K_h$ ), for various values of  $K_h$  (i.e. 0.1, 0.12, 0.144, 0.18, 0.2, 0.3, 0.4 and 0.5). It is observed from the developed fragility curve that as the  $K_h$  value increases, the  $P_f$  value decreases. A fragility curve can be used to calculate failure probability over a range of seismic zones, and for design purposes, a given seismic zone and probability of failure which determine a unique reliable side slope are selected. Furthermore, two machine learning (ML) models, namely Deep Neural Network (DNN) and Support Vector Regression (SVR) have been developed for the prediction of the factor of safety for different sides slope. The obtained correlation values (R) for SVR and DNN are approximately 0.95 and 0.82, respectively. With the help of the predicted factor of safety, the fragility curve against horizontal seismic coefficient are drawn for both SVR and DNN models. This aims to reduce the time of calculation and facilitate working by suggesting the best model for further analysis of railway embankment.

**Keywords:** *Fragility curve, Embankment, Machine learning, Probability of failure.*

## 1. Introduction

The quantitative examination of stability is required in the practice of civil engineering for a variety of technical issues, including the construction of railway embankments. The slope is vital in the stability of railway embankment slopes, since even the smallest collapse can result in severe financial losses and endanger lives. Engineers use the factor of safety value to determine how close or far the slope is from failure while analyzing the slope stability. To derive the factor of safety, the slope stability analysis of railway embankment is carried out for a 12.3 m height. The analysis has been performed using Bishop's method. There are several methods available to determine the factor of safety, namely Method of Slices, Jambu's method, Morgenstern method, soft computing methods, etc.

A fragility curve is a relationship that expresses the likelihood of a facility or component reaching or exceeding a precisely defined limit state as a function of some measure of environmental excitation [1]. Fragility curves have recently become more widely used in risk assessment for various damage stages of geotechnical structures [2,3]. These curves assess the total risk of infrastructures and provide an estimate of probable damage for a certain class. As a result, fragility curves can be utilized as a disaster decision-making tool, which is critical for disaster mitigation and emergency planning. Fragility functions describe the performance of structures and slope failure based on the conditional probability of failure for a particular range of loading condition. The reliability index calculated using these fragility function

is based on traditional probabilistic methodology, which can be seen as the relative probability of failure at a specific design point [4]. Many researchers have used various ways to quantify the fragility curve in previous studies [4,5,6,7,8,9].

Jeong and Elnashai (2007) categorized fragility curves into a variety of methods such as analytical, empirical, and hybrid approaches [11]. Even if each technique has its own set of drawbacks, the most widely discussed approaches in the literature are analytical ones. Because of their diversity, they can be divided into numerous categories depending on whether the used equation is an explicit or implicit function, and whether the likelihood of failure is calculated analytically or numerically [12]. The first-order reliability method (FORM) was frequently used to determine the reliability index and corresponding probability of failure. Vorogushyn et al. proposed the fragility curve development for earthen dikes using Monte Carlo simulation. Fotopoulou and Pitilakis (2013) suggested a method for constructing fragility curves for reinforced concrete buildings subjected to earthquake-induced landslides using the finite difference method [13]. To produce the fragility curve for embankments, Tsompanakis et al. (2012) incorporated the pseudo-static limit equilibrium method combined with Monte Carlo simulations. In this study, only one failure mechanism is investigated, and the correlation characteristic of fill material shear strengths is ignored.

The major goal of this study is to show the establishment of a methodology for railway embankment slope fragility functions in

\* Corresponding author. E-mail address: : [ranjandivesh453@gmail.com](mailto:ranjandivesh453@gmail.com) (D. Ranjan Kumar).

response to a variety of loading scenarios, e.g. earthquake and landslide events. Recent studies have introduced some novel developed techniques, such as the copula-based sampling method and FORM [11,12,13,14]. These strategies are incorporated to estimate the probability of failure of the embankment slope, accounting for the uncertainties of shear strength parameters. The developed fragility curves can be used to explore the diverse economic impacts of railway embankment failure, especially on transportation systems. To achieve the goal, data have been generated using Geo-studio 2012. To perform the stability analysis, SLOPE/W has been used with the Bishop's method. Moreover, two machine learning methods, DNN and SVR, have been also used to analyze the factor of safety. Finally, fragility curves are plotted for different embankment slopes for all the proposed models.

## 2. Methodology

All analysis are done for a railway embankment with a height of 12.293 m. The embankment is made up of C- $\phi$  type of soil. A cross-sectional view of the railway embankment is shown in Figure 1, and the material properties used in the embankment for each layer are presented in Table 1.

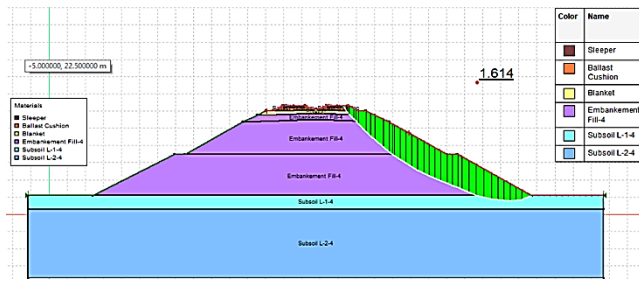


Figure 1. The railway embankment sectional view.

Table 1. The material properties of railway embankment.

Color	Name	Unit Weight (kN/m <sup>2</sup> )	Cohesion (kpa)	Phi (°)
	Sleeper	24	50	40
	Ballast Cushion	18	0	40
	Blanket	19	0	32
	Embankment Fill-4	25	17	34
	Subsoil L-1-4	25	20	30
	Subsoil L-2-4	24	21	27

The unit weight of the ballast cushion is taken as 18 KN/m<sup>2</sup>, and the unit weight of subsoil layer L-1-4 and embankment fill-4 are considered as 25 KN/M<sup>2</sup>. The detailed material properties and geometrical properties of railway embankment considered in this study are presented in Tables 1 and 2 respectively.

In this study, GeoStudio SLOPE/W has been used to perform the stability analysis with the Bishop's method. The input parameters used in this study are  $c$ ,  $\phi$ ,  $\gamma$ ,  $K_h$ , and  $K_v$  for calculating the factor of safety (FOS). Values of  $c$ ,  $\phi$ , and  $\gamma$  are entered in the material section,

while  $K_h$ , and  $K_v$  are entered in the loading section in SLOPE/W FOS is calculated for various side slopes, ranging from 1:2.0 to 1:1.5 for the side slope of embankment fill 1 and fill 2.

The horizontal seismic coefficient was determined by the IITK-GSDMA guideline for seismic design of earth dams and embankments [18] using equation (1), and the vertical horizontal seismic coefficient was calculated using equation (2) as follows:

$$K_h = \frac{ZIS}{3} \tag{1}$$

$$K_v = \frac{K_h}{2} \tag{2}$$

Where  $Z$  denotes the zone factor,  $I$  denotes the importance factor, and  $S$  denotes the shape factor. The values of  $Z$ ,  $I$ , and  $S$  for the corresponding zone factor are used as per IS-1893 (Part 1):2002, presented in Table 3.

Table 2. The illustration of Geometrical properties of embankment.

Geometrical Parameters	Value (m)
Total height of the embankment	12.293
The top width of the embankment	13.860
Height of the blanket layer	0.600
Height of prepared subgrade	1.000
Height of embankment fill 1	4.693
Height of embankment fill 2	6.000
Side slope of embankment fill 1	1.900
Side slope of embankment fill 2	1.900
Height of subsoil layer 1	2.000
Height of subsoil layer 2	10.000
Berm width at 6m level	1.5
Berm at subsoil layer 1	10

Table 3. The values of different factors.

Zone	Z	I	S	Kh
II	0.1	1.5	2.0	0.1
III	0.16	1.5	1.5	0.12
IV	0.24	1.5	1.2	0.144
V	0.36	1.5	1.0	0.18

For any specific value of  $K_h$ , the average value of FOS is considered as  $\mu$ , and the standard deviation of these FOS values is taken as  $\sigma$ .

The reliability index ( $\beta$ ) is defined as the shortest distance of the performance function from the origin of the reduced coordinate system of variables and can be calculated using the equation given below:

$$\beta = \frac{\mu - 1}{\sigma} \tag{3}$$

Where  $\beta$  represents the reliability index,  $\mu$  represents the mean of the factor of safety,  $\sigma$  represents the standard deviation of the factor of safety.

Then, to evaluate the  $P_f$  from these  $\beta$  values, an analytical expression is proposed [19–21] as follows:

$$P_f = 1 - \phi(\beta) \tag{4}$$

Here,  $\phi$  represents the standard normal cumulative distribution function.

## 3. Description of ML Techniques

### 3.1. Deep Neural Network (DNN)

An artificial neural network (ANN) model typically has three layers: one input layer, one hidden layer, and one output layer. A deep neural

network (DNN) is an ANN that has several layers between the input and output layers. The depth of the architecture is determined by the number of hidden layers. There are multiple nodes (i.e., neurons) and an activation function in each hidden layer. For different layers, activation functions may be different. Because of its extraordinary ability to understand intricate patterns and replicate non-linear circumstances in the real world, we use it as the meta-model to provide correct predictions. One input layer, three hidden layers, and one output layer make up the DNN structure. As a non-linear approximation, each hidden layer owns the rectified linear activation function (ReLU).

$$g(y) = \max(0, y) \quad (5)$$

In the output layer, there is no non-linear activation function. In the DNN, the number of neurons is equal in all the hidden layers and is calculated to give a specified total number of DNN parameters. Furthermore, the output of a hidden layer is connected to the input of the preceding layer, allowing the layers to learn the residual. These residual blocks help to simulate more complicated relationships by allowing it to dig deeper. Furthermore, inputs can experience quick feedforward propagation across layers via residual connections, and learning the residual mapping is simpler than the original mapping. The hidden layer of the DNN model is trained by randomly selected model parameters. The DNN model aims to reduce the loss function which is represented by mean-square error (MSE). Backward propagation of errors is an important step in fine-tuning DNN hyper parameters to solve the objective function accurately. In this study, gradient descent is used to update the weight of the DNN by back-propagating the measure of errors from the current layer to the previous layer. This process aims to predict values closer to the target output value. For loss optimization, the updated weight is calculated by equation (6).

$$W = w + \eta \times \frac{\partial E}{\partial w} \quad (5)$$

Where  $w$  represents the weight,  $\eta$  represents the learning rate, and  $E$  represents the error between the actual and predicted values. The DNN models are well-developed algorithms and for further details, please refer to [22,23].

### 3.2. Support Vector Regression (SVR)

Support vector regression is a popular choice for prediction and curve fitting for both linear and non-linear regression types. The SVR algorithm is based on the components of the SVM, in which support vectors are simply points closer to the created hyperplane in an  $n$ -dimensional feature space that separates the data points around the hyperplane.

There is a simple training set  $X = (x_i, y_i)$ , where  $(i = 1, 2, \dots, n)$ . A function  $f(x_i)$  is a regression function that can be written as:

$$f(x_i) = \omega * \phi(x_i) + b \quad (7)$$

Where  $x_i$  represent the input vector,  $x_i$  represent the target output vector,  $\omega$  belongs to any real number is called the weight vector,  $\phi(x_i)$  represent a non-linear mapping of the dataset within real number space to the higher feature space, and  $b$  represents the bias. The optimization can be done using the following function presented in Eq. (8).

$$\min \phi(\lambda) = \frac{1}{2}(\lambda^2) \quad (8)$$

$$\begin{cases} y_i - \lambda \cdot x_i - b \leq \varepsilon \\ \lambda \cdot x_i + b - y_i \leq \varepsilon \end{cases} \quad (9)$$

Where  $x_i$  and  $b$  are the normal vectors and offset of the regression function, respectively.

## 4. Data preparation

In this study, 100 random datasets are generated using GeoStudio by assuming the random values of cohesion ( $c = 0$  to 400), angle of friction ( $\phi = 0 - 38$ ), unit weight of soil ( $\gamma = 17 - 22$ ) for different values of  $K_h$  and  $K_v$  for all six varying slopes (i.e., slope 1:2.0 to 1:1.15).

The entire dataset used in this study is normalized between 0 to 1 using the following equation (9)

$$X_{Nor} = \frac{X_{Act} - X_{min}}{X_{max} - X_{min}} \quad (9)$$

Here  $X_{max}$  and  $X_{min}$  are the maximum and minimum values of the parameters, respectively.  $X_{Act}$  and  $X_{Nor}$  are the actual and normalized values of the parameters, respectively. After the process of normalization, the entire dataset is randomly divided into two parts i.e., training (70%) and testing (30%). The training dataset is used for the construction of the model, and the testing dataset is used for the validation of the model. Two Machine Learning (ML) techniques, Deep Neural Network (DNN) and Support Vector Regression (SVR), have been developed using these 100 datasets. Furthermore, 40 datasets have been generated using GeoStudio to validate the proposed ML model.

Ten statistical parameters such as the Coefficient of Determination ( $R^2$ ), Adjusted Determination Coefficient (AdjR<sup>2</sup>), Nash–Sutcliffe efficiency ( $NS$ ), Root Mean Square Error (RMSE), Variance Account Factor ( $VAF$ ), Performance Index ( $PI$ ),  $RMSE$ -observations standard deviation ratio ( $RSR$ ), Willmott's Index ( $WI$ ), Mean Absolute Error ( $MAE$ ), and Expanded Uncertainty ( $U_{95}$ ) were utilized to investigate the performance of the developed models. The mathematical equations of these statistical parameters are given below:

$$R^2 = \frac{\sum_{i=1}^n (x_i - x_{avg})^2 - \sum_{i=1}^n (x_i - y_i)^2}{\sum_{i=1}^n (y_i - y_{avg})^2} \quad (10)$$

$$AdjR^2 = 1 - \frac{(n-1)}{(n-p-1)}(1 - R^2) \quad (11)$$

$$NS = 1 - \frac{\sum_{i=1}^n (x_i - y_i)^2}{\sum_{i=1}^n (x_i - x_{mean})^2} \quad (12)$$

$$RMSE = \sqrt{\frac{1}{n} \sum_{i=1}^n (x_i - y_i)^2} \quad (13)$$

$$VAF = \left(1 - \frac{var(x_i - y_i)}{var(x_i)}\right) \times 100 \quad (14)$$

$$PI = adj. R^2 + (0.01 \times VAF) - RMSE \quad (15)$$

$$RSR = \frac{RMSE}{\sqrt{\frac{1}{n} \sum_{i=1}^n (x_i - x_{avg})^2}} \quad (16)$$

$$WI = \frac{\sum_{i=1}^n (x_i - y_i)^2}{\sum_{i=1}^n (|y_i - x_{mean}| + |x_i - x_{mean}|)^2} \quad (17)$$

$$MAE = \frac{1}{n} \sum_{i=1}^n |y_i - x_i| \quad (18)$$

$$U_{95} = 1.96(SD^2 + RMSE^2)^{\frac{1}{2}} \quad (19)$$

where  $x_i$  and  $y_i$  represent the experimental and observed  $i$ th value,  $n$  corresponds to the size of dataset samples,  $x_{avg}$  is the average of the experimental value, and  $P$  represents the number of input parameters. The  $U_{95}$  (Eq. 19) provides uncertainty up to a 95% confidence level, with 1.96 being subsequent to the confidence level coverage factor.

## 5. Result and discussion

This section presents the results of the proposed DNN and SVR models in the development of fragility curve and the determination of probability of failure for different railway embankment side slopes such as 1:1.5, 1:1.6, 1:1.7, 1:1.8, 1:1.9, and 1:2.0. The outcomes of all proposed models are shown in the following sub-sections. Finally, the best predictive model was determined through the proposed statistical parameters.

### 5.1. Statistical parameters

In this section, ten statistical parameter values were computed to analyze and compare the accuracy of the proposed models corresponding to various slopes. The statistical parameters include Coefficient of Determination ( $R^2$ ), Adjusted Determination Coefficient (AdjR<sup>2</sup>), Nash–Sutcliffe efficiency ( $NS$ ), Root Mean Square Error

(RMSE), Variance Account Factor (*VAF*), Performance Index (*PI*), *RMSE*-observations standard deviation ratio (*RSR*), Willmott's Index (*WI*), Mean Absolute Error (*MAE*), and Expanded Uncertainty (*U<sub>95</sub>*). To assess the accuracy of ML-based models, many researchers employ all these statistical parameters[24–30]. The parameters calculated for both models for various slopes are considered the best, because the obtained values are close to their ideal value. The results obtained from the performance evaluation of the proposed ML models are presented in Table 4.

**5.2. Scatterplot**

The results of the different proposed models are presented through scatterplots which represent the normalized actual output versus the normalized predicted output. method illustrates the accuracy of the proposed models by plotting the actual and predicted data along the line ( $x = y$ ). Data points located on the line ( $x = y$ ) represent the best predictive model. The scatterplots of training (Figure 2a, c, e, g, I, and k), and testing (Figure 2b, d, f, h, j, and l) are plotted separately for both the DNN and SVR models. It can be observed from the scatterplots of

the proposed models that the plotted points are located close to the line ( $x = y$ ), implying a successful prediction of all models.

**5.3. Fragility curves**

It is necessary to address the responses for slopes using a traditional deterministic limit equilibrium analysis and ML technique to create analytical fragility curves. In this step, a fragility curve was created according to the dynamic simulations. Figure 3 (a-l) represent the fragility curves for both the actual dataset and model dataset for six different slopes. The comparison between the fragility curve obtained from the actual output and the developed DNN and SVR models for different embankment slopes is presented in Figure. 3 (a, c, e, g, I, k) for the DNN model and Figure. 3 (b, d, f, h, j, l) for the SVR model. It can be seen that as the value of the horizontal seismic coefficient increases, the probability of failure also increases. In addition, the slope of the curves can also play an important role in the failure of railway embankments. it can also be observed from the curves that the probability of failure is lower for slope 1:2.0 in comparison to slopes 1:1.5, 1:1.6, 1:1.7, 1:1.8, and 1:1.9.

**Table 4.** The statistical Parameters.

Statistical parameters	Slope 1:2.0		Slope 1:1.9		Slope 1:1.8		Slope 1:1.7		Slope 1:1.6		Slope 1:1.5	
	DNN	SVR										
<i>R</i> <sup>2</sup>	0.899	0.909	0.953	0.460	0.959	0.832	0.898	0.936	0.841	0.581	0.870	0.8574
<i>Adj R</i> <sup>2</sup>	0.894	0.904	0.950	0.431	0.957	0.823	0.892	0.932	0.832	0.558	0.863	0.8497
<i>NS</i>	0.179	-0.125	0.306	0.047	-0.240	-0.223	-0.209	-0.460	-0.284	-0.536	-0.634	-0.5667
<i>RMSE</i>	0.241	0.283	0.224	0.262	0.303	0.301	0.301	0.330	0.310	0.339	0.351	0.3437
<i>VAF</i>	49.116	39.375	72.341	44.248	61.476	58.600	52.243	57.156	60.770	42.537	32.243	52.5169
<i>PI</i>	1.144	1.015	1.450	0.611	1.269	1.108	1.114	1.173	1.130	0.645	0.835	1.0312
<i>RSR</i>	0.906	1.061	0.833	0.976	1.114	1.106	1.100	1.208	1.133	1.239	1.278	1.2517
<i>WI</i>	0.654	0.607	0.760	0.690	0.663	0.663	0.638	0.632	0.663	0.610	0.559	0.6168
<i>MAE</i>	0.209	0.237	0.195	0.198	0.258	0.257	0.258	0.287	0.267	0.279	0.295	0.2970
<i>U<sub>95</sub></i>	0.255	0.290	0.261	0.301	0.322	0.322	0.314	0.345	0.332	0.354	0.355	0.3572

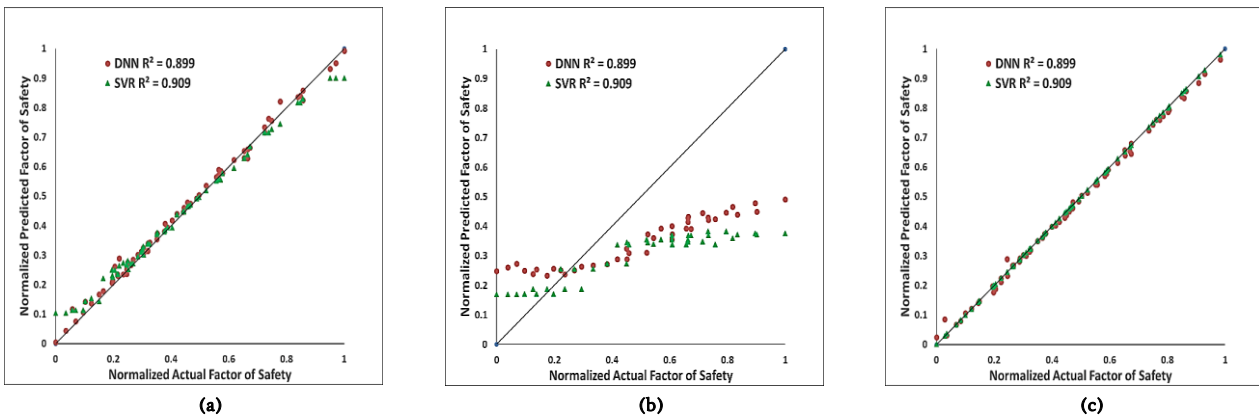


**Figure 2** a, c, for the training phase and Figure 2b for the Testing phase.

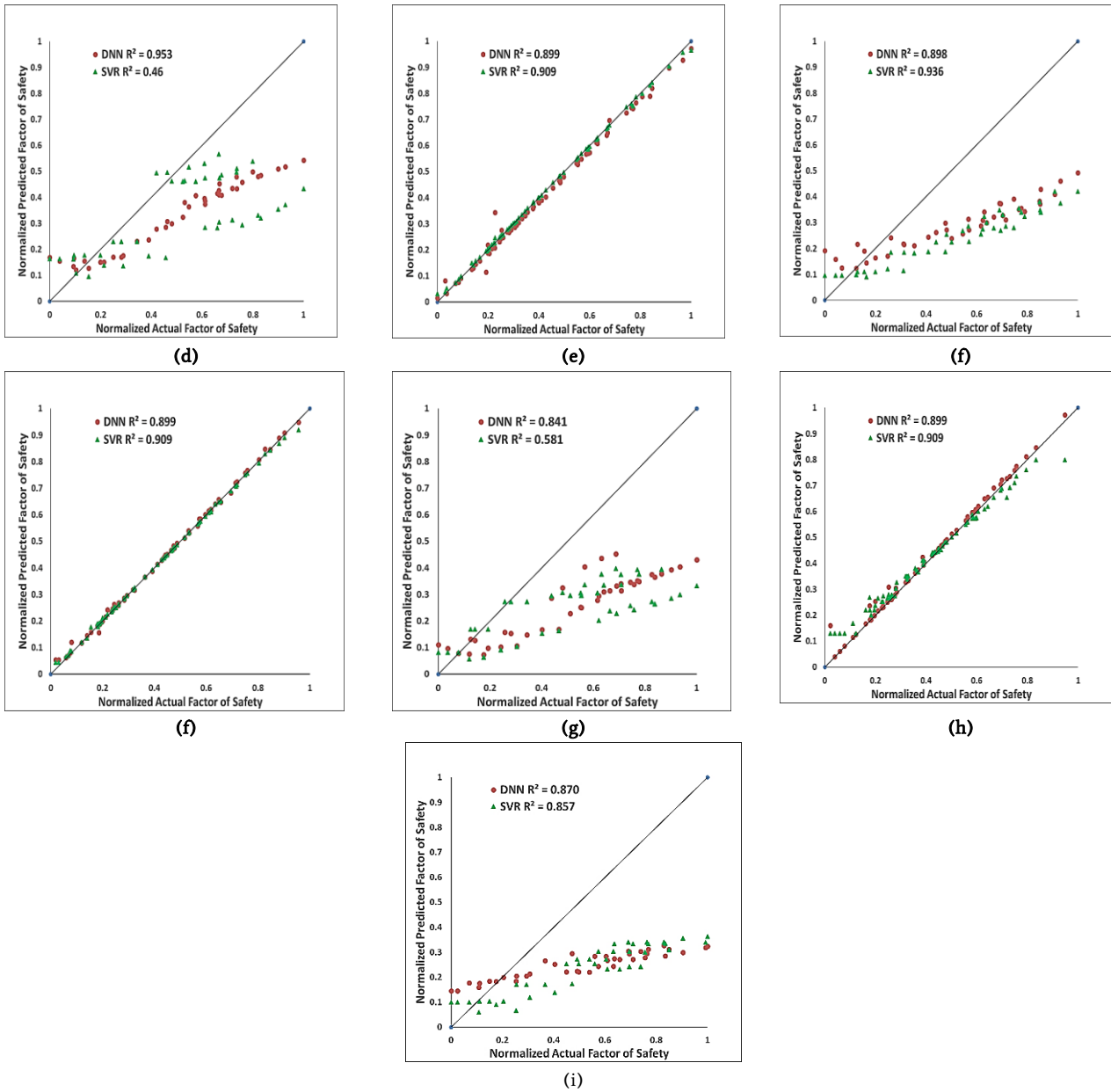


Figure 2 e, g, I, k) for the training phase and Figure 2 d, f, h, j, l) for the Testing phase.

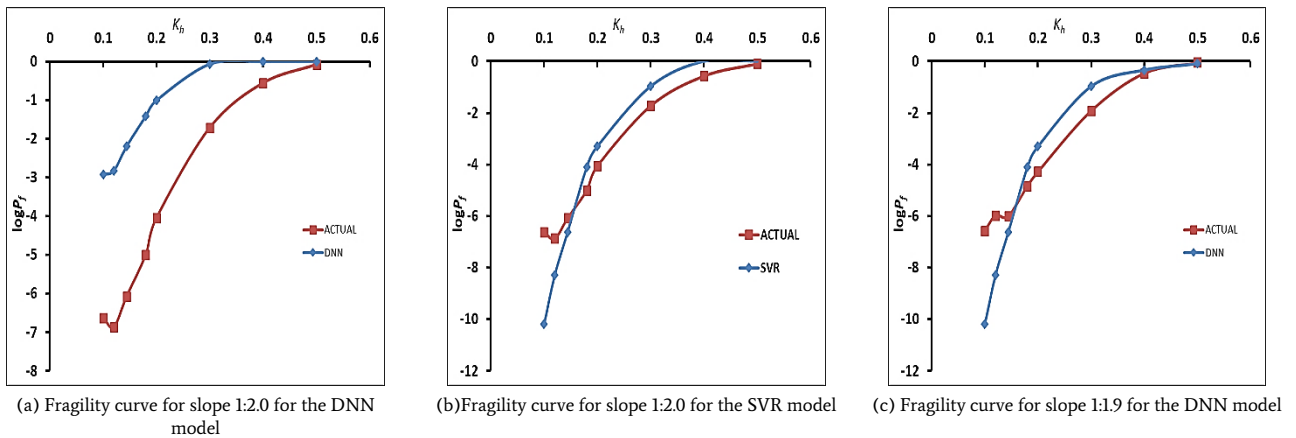


Figure 3 (a-c). The illustration of fragility curve for all models with different slopes.

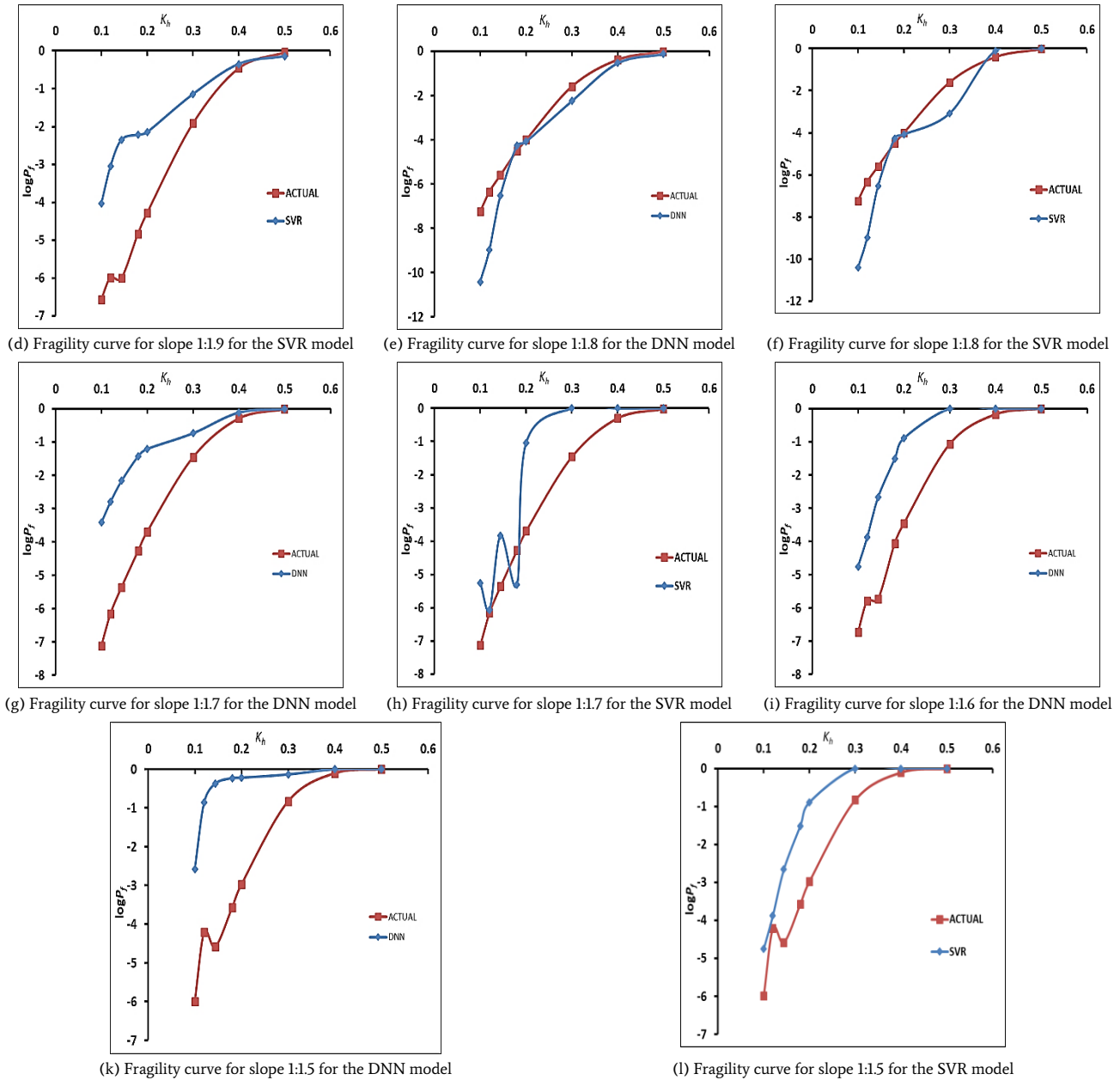


Figure 3 (d-l): The illustration of fragility curve for all models with different slopes.

## 6. Conclusion

This study demonstrates the application of the machine learning methodology in developing fragility curves for railway embankments. The factor of safety of the railway embankment of various slopes was estimated in this investigation using the traditional, well-proven reliability methods. The shear strength properties of landfill materials and slope geometries significantly influenced the fragility curves generated by the FORM and machine learning models. For instance, fragility curves during seismic excitations are directly correlated with the magnitude of the earthquake, as the magnitude increases, the probability of failure also increases. Additionally, when slope height increases, fragility curves alter, showing that slopes with a higher slope height have a larger failure chance. The calculated probability of failure is also impacted by changes in inclination. The results of this work demonstrated that the slope responses can be more thoroughly interpreted using the fragility analysis under a wide range of loading conditions. It is thus suggested that the analysis of the railway

embankment's fragility curve can provide a better estimation of the probability of failure. In general, the novel interpretable model based on DNN and SVR developed in this work is suitable and efficient; it offers benefits and prospects for analyzing the contribution of influencing elements to the failure of railway embankments. Following the prediction, the model was analyzed using some statistical parameters, and the best models for the prediction of the safety factor were chosen by comparing them. The statistical parameters and numerous graphs, including the actual vs expected curve and fragility curve, were used to study these comparisons. The  $R^2$  values for DNN and SVR showed good accuracy in both the training and testing phases presented in Table 4. The proposed DNN and SVR models have high potentials to predict factors of safety and can be used as quick tools in railway embankment analysis.

## REFERENCES

- [1] Porter K. A beginner's guide to fragility, vulnerability, and risk. University of Colorado Boulder, 119 pp 2019.
- [2] Martinović K, Reale C, Gavin K. Fragility curves for rainfall-induced shallow landslides on transport networks. *Can Geotech J* 2018;55:852–61. <https://doi.org/10.1139/cgj-2016-0565>.
- [3] Wu XZ. Development of fragility functions for slope instability analysis: Fragility functions for slope instability analysis. *Landslides* 2015;12:165–75. <https://doi.org/10.1007/s10346-014-0536-3>.
- [4] Kennedy RP, Cornell CA, Campbell RD, Kaplan S, Perla HF. Probabilistic seismic safety study of an existing nuclear power plant. *Nucl Eng Des* 1980;59:315–38.
- [5] Gardoni P, Der Kiureghian A, Mosalam KM. Probabilistic capacity models and fragility estimates for reinforced concrete columns based on experimental observations. *J Eng Mech* 2002;128:1024–38.
- [6] Jeong S-H, Elnashai AS. Probabilistic fragility analysis parameterized by fundamental response quantities. *Eng Struct* 2007;29:1238–51.
- [7] Ebeling RM, Fong MT, Chase A, Arredondo E. Fragility analysis of a concrete gravity dam and its system response curve computed by the analytical program GDLAD\_Sloping\_Base 2008.
- [8] Vorogushyn S, Merz B, Apel H. Development of dike fragility curves for piping and micro-instability breach mechanisms. *Nat Hazards Earth Syst Sci* 2009;9:1383–401.
- [9] Schultz MT, Gouldby BP, Simm J. Beyond the factor of safety developing fragility curves to characterize system reliability 2010.
- [10] Kennedy RP, Cornell CA, Campbell RD, Kaplan S, Perla HF. Probabilistic seismic safety study of an existing nuclear power plant. *Nucl Eng Des* 1980;59:315–38. [https://doi.org/10.1016/0029-5493\(80\)90203-4](https://doi.org/10.1016/0029-5493(80)90203-4).
- [11] Jeong SH, Elnashai AS. Probabilistic fragility analysis parameterized by fundamental response quantities. *Eng Struct* 2007;29:1238–51. <https://doi.org/10.1016/j.engstruct.2006.06.026>.
- [12] Schultz MT, Gouldby BP, Simm JD, Wibowo JL. Beyond the Factor of Safety : Developing Fragility Curves to Characterize System Reliability-US Army Corps of Engineers 2010:51.
- [13] Fotopoulou SD, Ptilakis KD. Vulnerability assessment of reinforced concrete buildings subjected to seismically triggered slow-moving earth slides. *Landslides* 2013;10:563–82.
- [14] Wu XZ. Probabilistic slope stability analysis by a copula-based sampling method. *Comput Geosci* 2013;17:739–55.
- [15] Hasofer AM, Lind NC. Exact and invariant second-moment code format. *J Eng Mech Div* 1974;100:111–21.
- [16] Zahn JJ. Empirical failure criteria with correlated resistance variables. *J Struct Eng* 1990;116:3122–37.
- [17] Low BK, Tang WH. Efficient spreadsheet algorithm for first-order reliability method. *J Eng Mech* 2007;133:1378–87.
- [18] Dash, S.R. and Jain SK. IITK-GSDMA Guidelines for seismic design of buried pipelines: provisions with commentary and explanatory examples. National Information Center of Earthquake Engineering, Kanpur, India. Indian Inst Technol Kanpur 2007.
- [19] Frangopol DM. Probability concepts in engineering: emphasis on applications to civil and environmental engineering. vol. 4. John Wiley & Sons Incorporated; 2008. <https://doi.org/10.1080/15732470802027894>.
- [20] Chowdhury R, Flentje P. Role of slope reliability analysis in landslide risk management. *Bull Eng Geol Environ* 2003;62:41–6. <https://doi.org/10.1007/s10064-002-0166-1>.
- [21] Kumar DR, Samui P, Burman A, Kumar S. Seismically Induced Liquefaction Potential Assessment by Different Artificial Intelligence Procedures. *Transp Infrastruct Geotechnol* 2023;1–22.
- [22] Goodfellow I, Bengio Y, Courville A, Bengio Y. Deep learning [http://www.deeplearningbook.org]. MIT Press Cambridge, MA 2016.
- [23] Kumar R, Kumar A, Ranjan Kumar D. Buckling response of CNT based hybrid FG plates using finite element method and machine learning method. *Compos Struct* 2023;319:117204. <https://doi.org/10.1016/j.compstruct.2023.117204>.
- [24] Kumar DR, Samui P, Wipulanusat W, Keawsawavong S, Sangjinda K, Jitchaijaroen W. Soft Computing Techniques for Predicting Penetration and Uplift Resistances of Dual Pipelines in Cohesive Soils. *Eng Sci* 2023. <https://doi.org/10.30919/es897>.
- [25] Kumar DR, Samui P, Burman A. Suitability assessment of the best liquefaction analysis procedure based on SPT data. *Multiscale Multidiscip Model Exp Des* 2023;1–11.
- [26] Kumar DR, Samui P, Wipulanusat W, Keawsawavong S, Sangjinda K, Jitchaijaroen W. Soft-Computing Techniques for Predicting Seismic Bearing Capacity of Strip Footings in Slopes. *Buildings* 2023;13. <https://doi.org/10.3390/buildings13061371>.
- [27] Kumar DR, Samui P, Wipulanusat W, Keawsawavong S, Sangjinda K, Jitchaijaroen W. Bearing Capacity of Eccentrically Loaded Footings on Rock Masses Using Soft Computing Techniques. *Eng Sci* 2023;24:929.
- [28] Kumar DR, Samui P, Burman A, Wipulanusat W, Keawsawavong S. Liquefaction susceptibility using machine learning based on SPT data. *Intell Syst with Appl* 2023;20:200281. <https://doi.org/10.1016/j.iswa.2023.200281>.
- [29] Kumar M, Biswas R, Kumar DR, Samui P, Kaloop MR, Eldessouki M. Soft computing-based prediction models for compressive strength of concrete. *Case Stud Constr Mater* 2023;19:e02321.
- [30] Kumar M, Biswas R, Kumar DR, Pradeep T, Samui P. Metaheuristic models for the prediction of bearing capacity of pile foundation. *Geomech Eng* 2022;31:129–47. <https://doi.org/10.12989/gae.2022.31.2.129>.